Geophysical characterization of the near-surface at Priddis, Alberta

J. Helen Isaac, Lei Zhi, Malcolm B. Bertram, Don C. Lawton, and L. R. Bentley

ABSTRACT

We integrated well data with seismic reflection and refraction data and electrical resistivity data acquired at the same time as the refraction data on the University of Calgary lands at Priddis, Alberta, in 2012. The purpose was to derive a model of the near-surface so that we might predict the lithology to be encountered in wells that were planned to be drilled in the autumn of 2013 for the installation of a permanent downhole seismic recording and monitoring system.

There is a good match between the velocity model derived from the refraction survey, the interpretation of reflectors on the reflection data, the existing Rothney test well lithology and the electrical resistivity inversion. A sandstone penetrated between 65 m and 90 m in the Rothney observation test well was predicted to be encountered updip between about 25 m and 50 m in Well 1, drilled in October, 2013. Well 1 turned out to have three sandstones within this interval: at 23-28 m, 31-37 m and 46-50 m. A major resistive unit, interpreted to be a sandstone, correlates to strong reflectors on the reflection seismic data and a relatively high velocity on the seismic refraction data. We predicted that the top of this unit would be encountered at about 95 m depth in Well 1. Our predictions turned out to be accurate as Well 1 penetrated a sandstone from 91-102 m. A hard shale with sandstone ledges was penetrated at 124 m in Well 1 and slowed the drilling of the well. It projects onto the observation well deeper than the total depth. It correlates to a high amplitude reflection on the seismic data.

METHOD

The refraction seismic line and electrical resistivity line were coincident, with the resistivity line being little longer to both the east and the west. The reflection line was located about 220 m to the south of these (Figure 1). The regional strike direction is 20° west of geographic north (GSC, 1941).

Seismic data

A seismic reflection survey was acquired in July, 2012, and a seismic refraction survey was acquired in September, 2012, both using a mini-vibroseis source, the CREWES IVI Envirovibe, and 3C SM7 geophones. For both surveys the Aries recording system was employed. The survey details are listed in Table 1. Figure 2 is a photograph of the field layout for the reflection survey with flags showing geophone locations and the ruts defining the path of the vibroseis truck, which was about 8 m away from the receiver line.

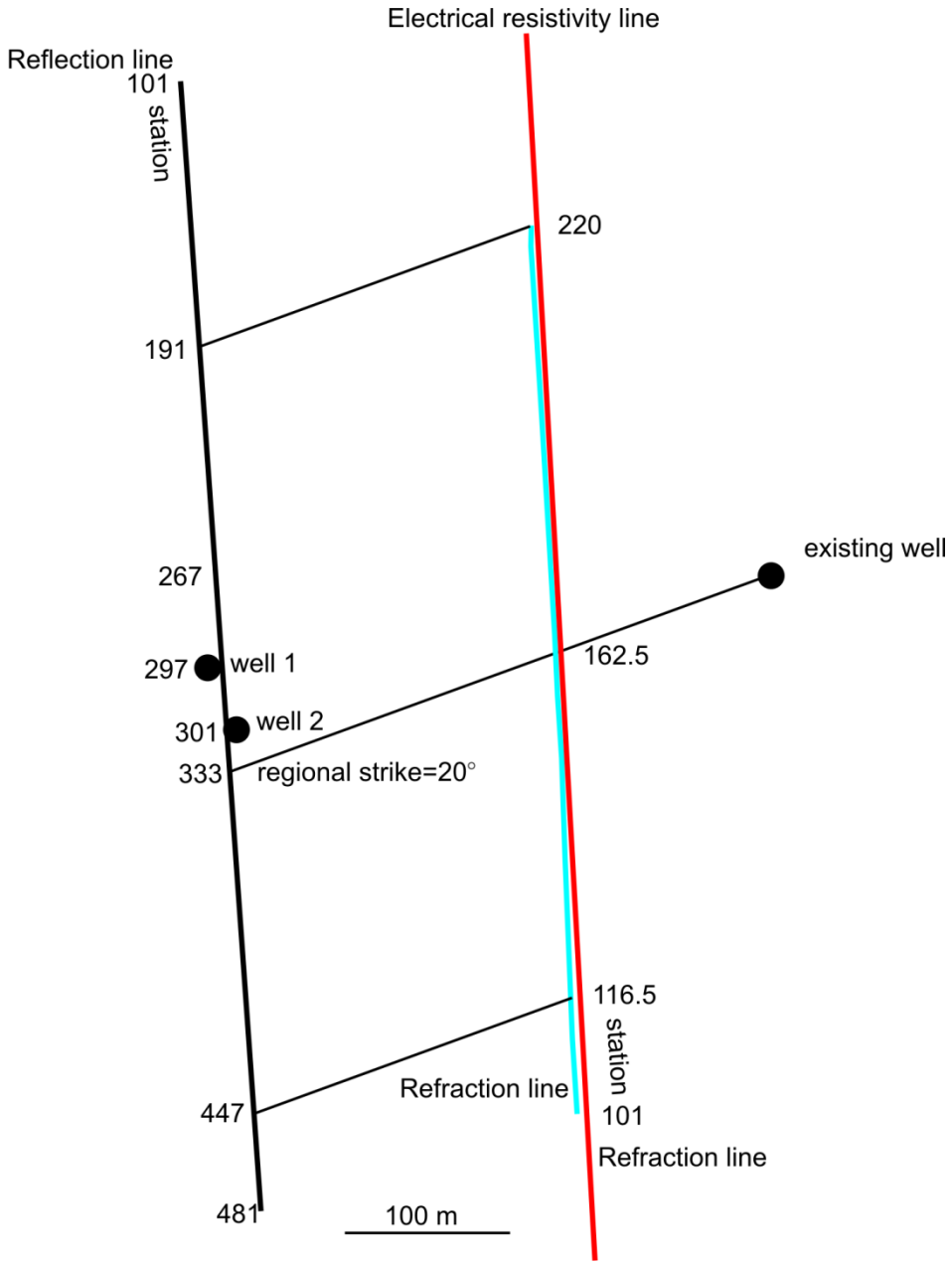

FIG. 1: Layout of the seismic reflection line (black), seismic refraction line (blue) and electrical resistivity line (red). Wells 1 and 2 were drilled in October, 2013.

Table 1. Seismic data acquisition parameters.

	Reflection survey	Refraction survey
Source sweep	10-120 Hz	10-200 Hz
Source number and spacing	96 at 8 m	59 at 10 m
Receiver number and spacing	392 at 2 m	120 at 5 m
Correlated data recording time	3 s	3 s
Line length	778 m	591 m

FIG. 2: Layout of the reflection seismic survey at Priddis. Flags show the geophone locations and the ruts show the route of the vibroseis truck.

Examples of field shots and their spectra are shown in Figure 3. An AGC has been applied to the data for display. The field data are dominated by high amplitude, low frequency surface waves which are source-generated. These wavetrains are attenuated through processing.

We picked first breaks on the refraction data and calculated refraction statics using a generalized reciprocal method inversion algorithm (Palmer, 1981). A near-surface velocity-depth model was obtained through this inversion. The depths and velocities obtained through the refraction analysis (Figure 4) are adequate for showing general trends but the absolute values are unreliable, as they change somewhat depending on the offset range chosen for the analysis.

We processed stacked and post-stack time migrated the reflection data (Figure 5). Reflectors that dip to the east can be seen clearly on this section. This dip is consistent with the 30° dip mapped on geology maps and seen in outcrop along the hill to the west of the field area (GSC, 1941; Isaac and Lawton, 2011).

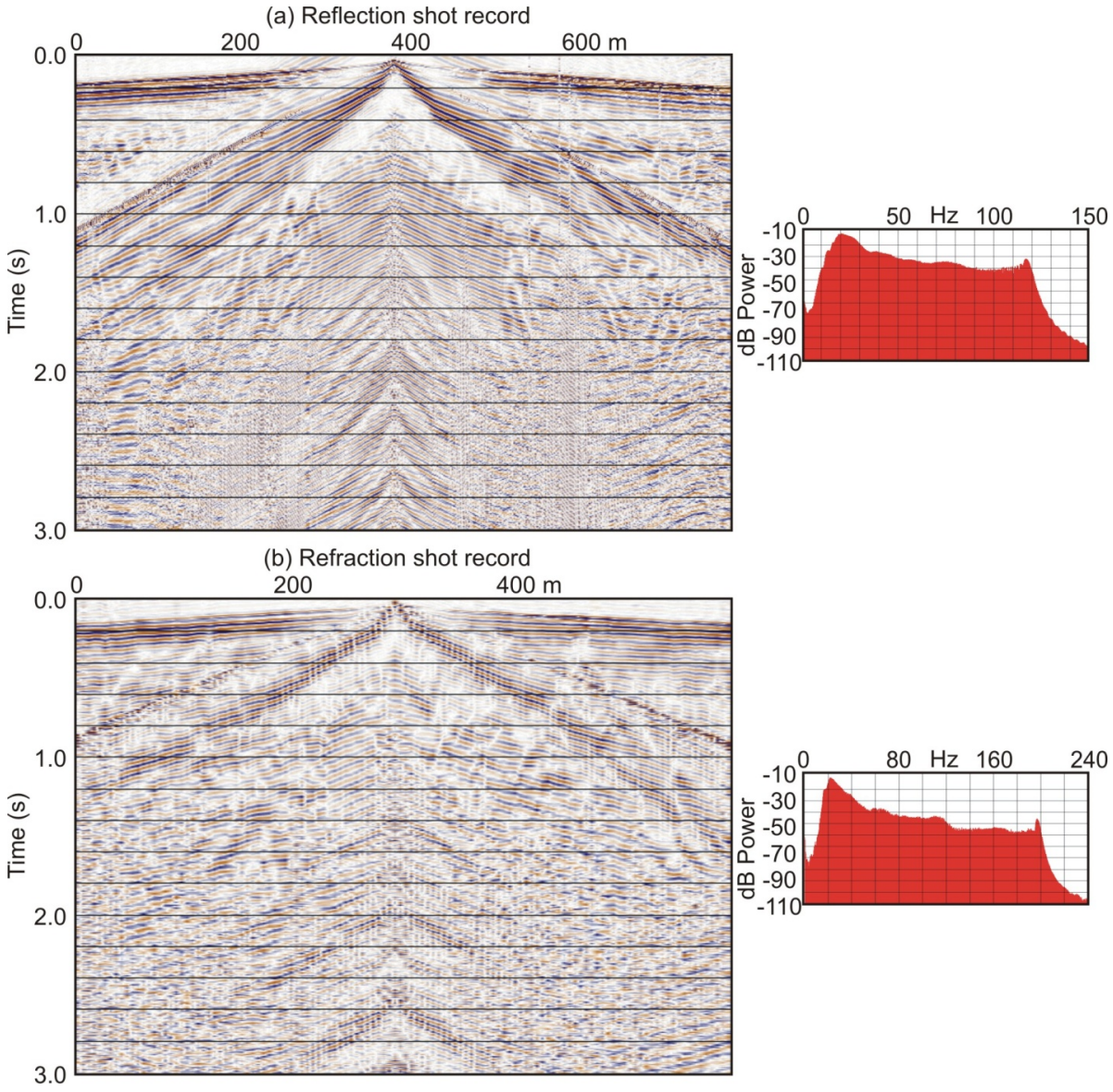

FIG. 3: Field shots and their spectra from the (a) reflection survey and (b) refraction survey.

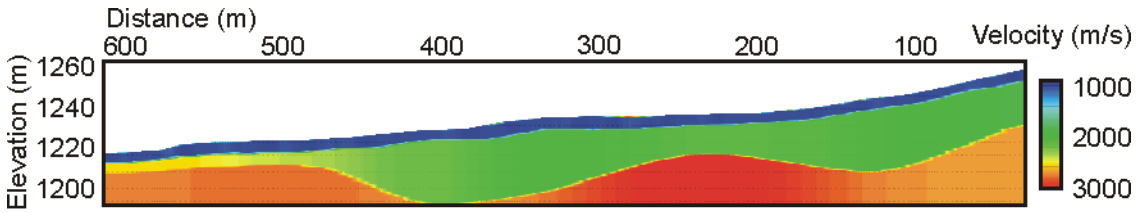

FIG. 4: Refraction velocity model derived through inversion of first break picks.

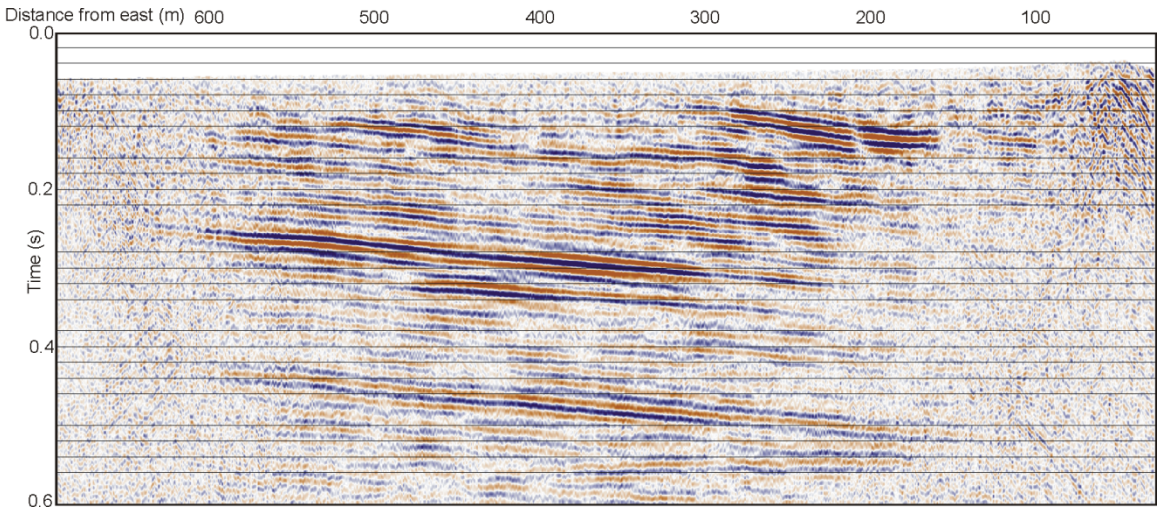

FIG. 5: Post-stack time migrated seismic reflection line.

Electrical resistivity data

The electrical resistivity line was coincident with the refraction line although a little longer to both the east and the west.

The acquisition instrument for collecting electrical resistivity tomography data was the IRIS Syscal Pro Switch 72. The 72 multi-channel system has 12 cables with a control box in the middle, and five connectors on each side of the control box to connect every two cables. The sequence used for acquiring data was a pre-defined dipole-dipole electrode array, which included approximately 40% reciprocal measurements. For the resistivity line, we first used a 10 m unit electrode spacing, resulting in a total spread length of 710 m. Later a 5 m unit electrode spacing was used with 72 electrodes, utilizing three cable "rolls", for a total spread length of 715 m. The two different unit electrode spacings, 5 m and 10 m, were used to improve data density and both vertical and horizontal resolution in the near surface and to achieve a maximum depth of investigation.

We processed the resistivity data using the RES2DINV program, which runs a smoothness-constrained Gauss-Newton least-squares inversion (Sasaki, 1992; Loke, 2000; Geotomo, 2013). Prior to inverse modelling, noisy data and bad data points were edited from the pseudo-section to ensure high ERT data quality. A post-inversion RMS cut-off approach was also utilized to assure a good convergence between the calculated and measured apparent resistivities.

Forward modelling utilized the finite-element method to adjust the node positions to follow the topography. We chose parameters to minimize the error generated by the forward modelling algorithm: four computational nodes between adjacent electrodes and finest vertical mesh size. In addition, the cell size was set to half of the unit electrode spacing to achieve a finer model. An L1 norm constraint was applied to both the data and the model to minimize the difference between the calculated and measured resistivities.

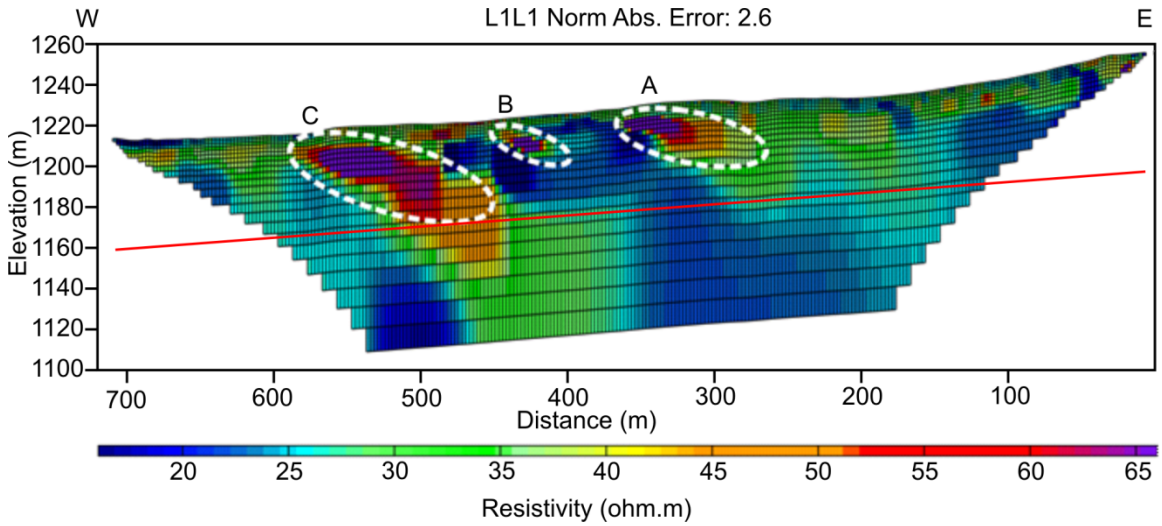

FIG.6: Combined 5 m and 10 m unit electrode spacing apparent resistivity tomogram, 5th iteration.

The approximate reliable depth of investigation, based on model resolution, is given by the red solid line in Figure 6, which is about 60 m deep. Overall, the resistivity ranges from 16 to 66 ohm.m, and the entire pseudosection is relatively conductive. The tomogram shows that the depth to the bedrock is about 5 m and that the upper bedrock is highly heterogeneous and dominated by sandstone and mudrocks. Three major anomalies (outlined by dashed white circles and labelled as A, B and C in Figure 6) are located at horizontal distances 280-360 m, 415-440 m, and 450-580 m. These are interpreted to be sandstones within the bedrocks, as they tend to be very resistive (> 52 ohm.m, red-to-purple colour).

Well data

A shallow well was drilled at Priddis in 2007 (Wong et al., 2007). The depth of the well is 137 m, which enables it to be classified as a water well, according to Energy Resources Conservation Board (ERCB) guidelines. The well penetrated clastic rocks of the Palaeocene Paskapoo Formation. A major sandstone was encountered between 65 and 89 m depth, with minor, thin sandstones in the section above (Figure 7). The sonic log shows an increase in seismic velocity at the top of the sandstone and a decrease at the base. The synthetic seismogram, plotted in Figure 7 in depth, indicates a strong negative seismic response at the sand/shale interface at the base of the sandstone and a less definitive positive event at the top of the sandstone because of interference from earlier seismic reflections. The minor sandstones are too thin to be resolved by our seismic data.

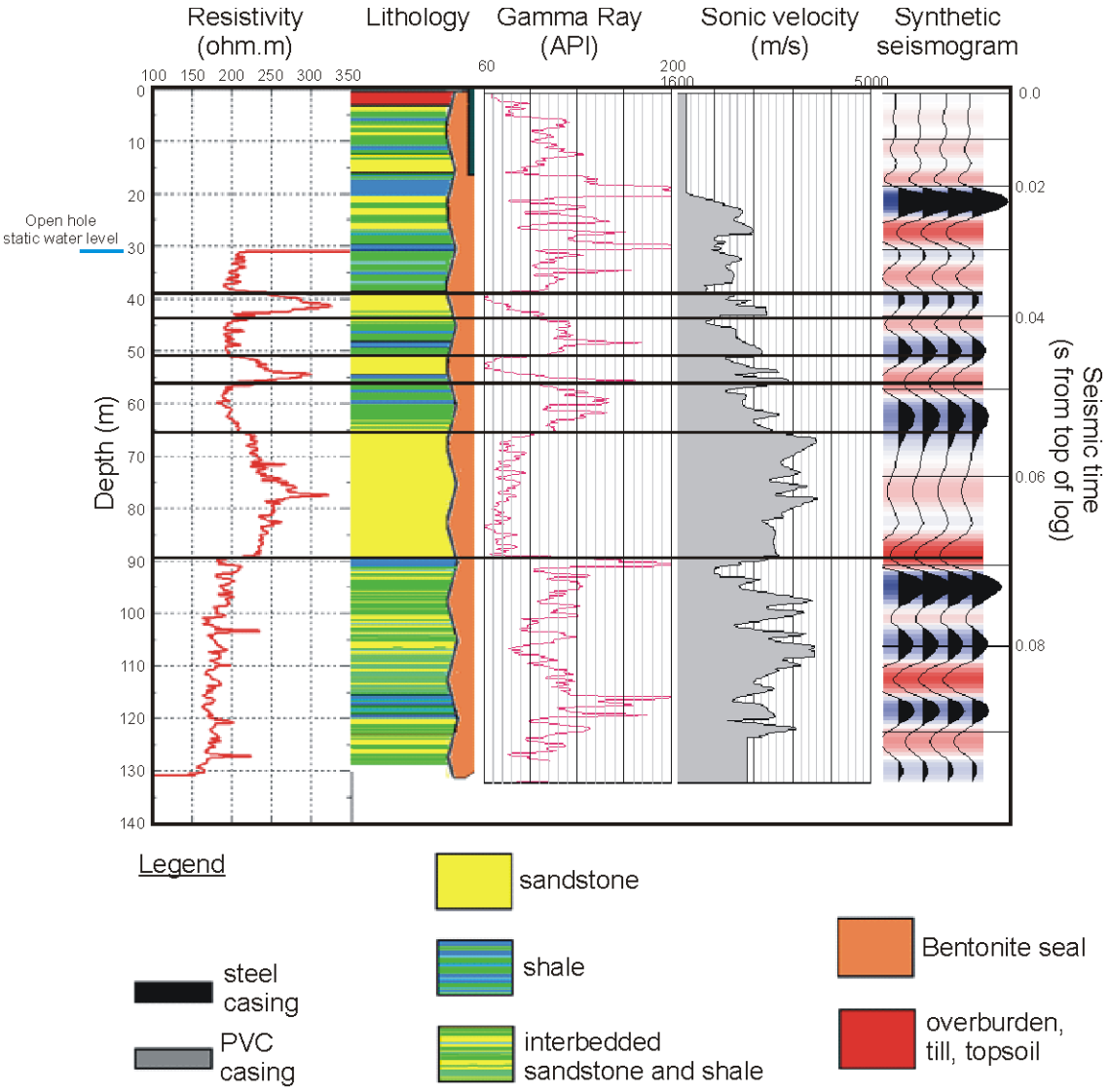

FIG. 7: The existing Rothney observation test well (partly from Wong et al., 2007).

We created a synthetic seismogram from the velocity data of the Rothney test well and tied it to the post-stack time migrated seismic reflection data (Figure 8). The tie was not easy to make as there is no sonic velocity for the top 20 m and the seismic data are too poor in the shallow section to tie many reflectors. We estimated a velocity for the top 20 m from the refraction velocity information. We picked the base of the major sandstone seen in the Rothney test well as a fairly weak red trough just above 80 ms at the location of the well in Figure 8. The top of the sandstone is not well represented on the seismic data.

We used this correlation of synthetic seismogram to seismic section in the time domain to guide our correlation and interpretation in the depth domain. The time section was converted to depth using the near-surface velocity model.

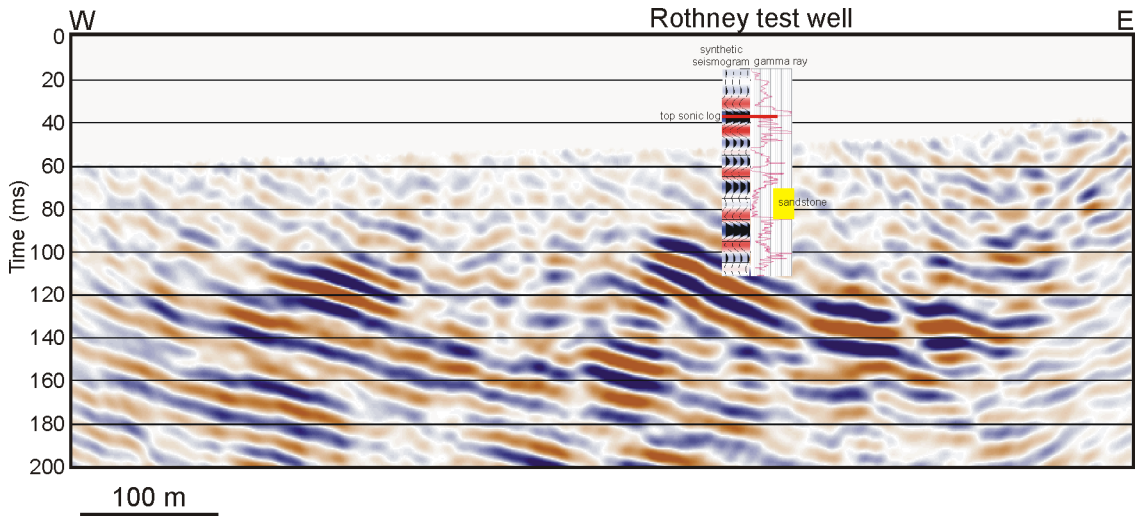

FIG. 8: Tie between time migrated seismic data and a synthetic seismogram from the Rothney test well sonic log. The well is projected along strike onto the line.

INTEGRATION OF RESULTS

All the geophysical data are plotted in Figure 9, separately at first (Figure 9a) then superimposed on each other (Figure 9b) with the well lithology and a synthetic seismogram in depth added. The seismic refraction line and electrical resistivity profile were projected about 215 m along strike and the Rothney test well was projected about 345 m along strike to the surface location of the reflection line.

The sandstone encountered between 60 and 95 m in the Rothney test well is indicated by the shallowest yellow band in Figure 9. It correlates to a small, shallow resistive unit at about 430 m on the electrical resistivity profile.

Bright reflectors dipping to the east between surface locations 350 m and 100 m and between elevations of about 1130 m to 1050 m correlate with a strong resistive (red) unit observed between 500 m and 600 m on the electrical resistivity data. They also correspond fairly well to a high velocity unit in the refraction survey (in orange). We interpret these to be geophysical responses to a sandstone.

The low resistivity in dark blue centred around 400 m correlates to an area of poor reflectivity on the reflection seismic data and low velocity (green) on the refraction velocity model so is interpreted to be the response to a shale. Outcrops are hard to see in the field because of vegetation cover. It would be interesting to see if there are any variations in vegetation indicating sandstones or shales.

From these integrated data we predicted the stratigraphy to be encountered in Well 1 drilled in October, 2013. In Figure 10 we plot the location of Well 1 on an enlarged portion of the integrated data presented in Figure 9b. We predicted that the major sandstone encountered in the Rothney test well would be penetrated in Well 1 from about 25 m to 50 m below the surface. We also predicted that a resistive sandstone would be encountered at around 95 m depth below the surface.

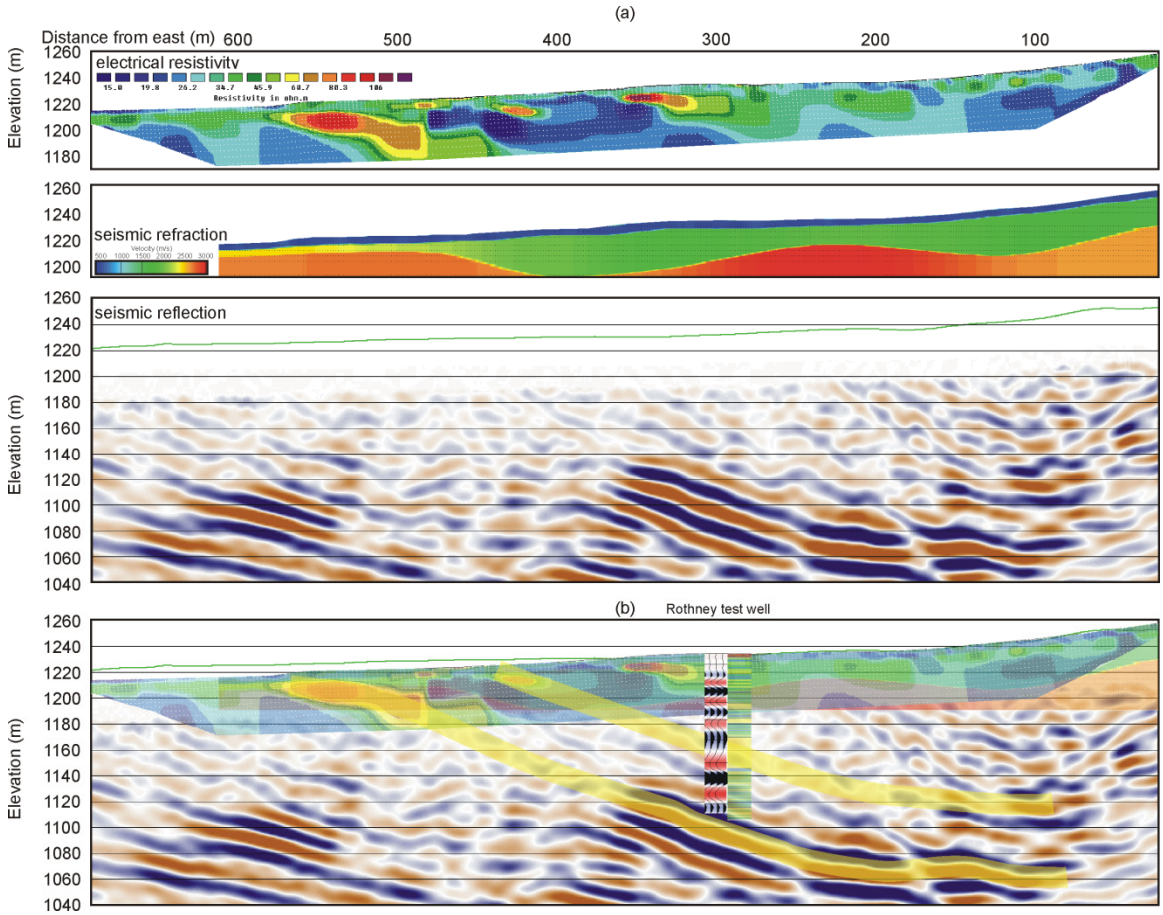

FIG. 9: Electrical resistivity profile, seismic refraction near-surface velocity model and seismic reflection data plotted separately (a) and then superimposed (b) with the Rothney observation well lithology and the synthetic seismogram in depth added. The refraction and electrical resistivity data were shifted laterally along strike to align locations.

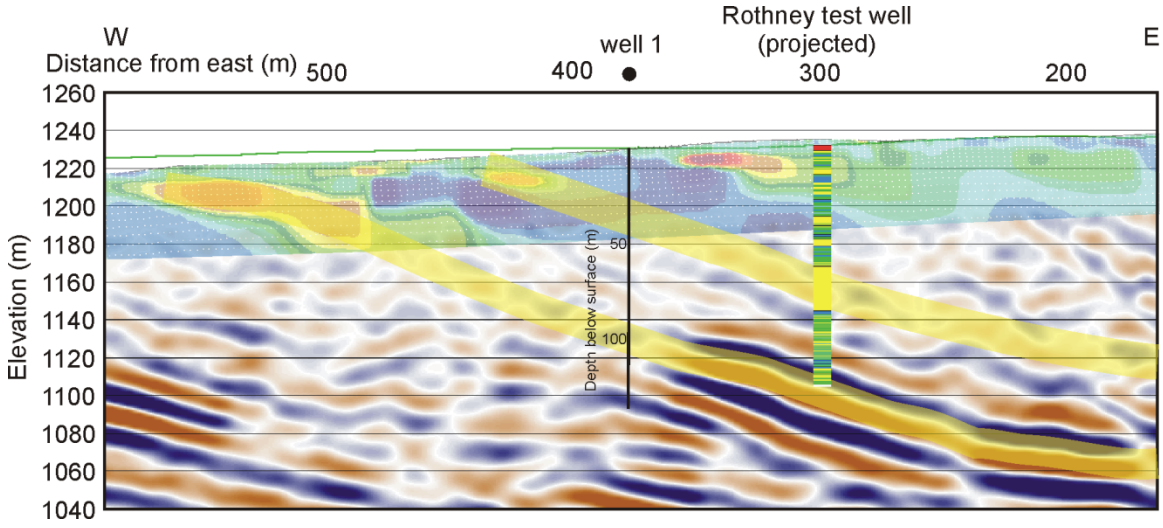

FIG. 10: Zoom of Figure 9b with the location of well 1, and predicted sandstones in yellow.

POSTLUDE

Figure 11 shows the lithology in well 1, obtained from the drilling report, overlain on Figure 10. No logs have been obtained yet and the core has not been analysed. Well 1 encountered grey sandstones from 23-28 m, 31-37 m and 46-50 m, which we correlate to the sandstone encountered between 65 and 90 m in the original Rothney test well. An 11-m thick sandstone was found at 91-102 m and correlates to the resistive sandstone we predicted from the seismic character and electrical resistivity to be entered at 95 m depth.

The drillers encountered a very hard unit, described as a shale with sandstone ledges, at about 125 m depth, which slowed the drilling considerably. This we correlate to a high amplitude reflection on the seismic data which was below the TD of the original Rothney observation well.

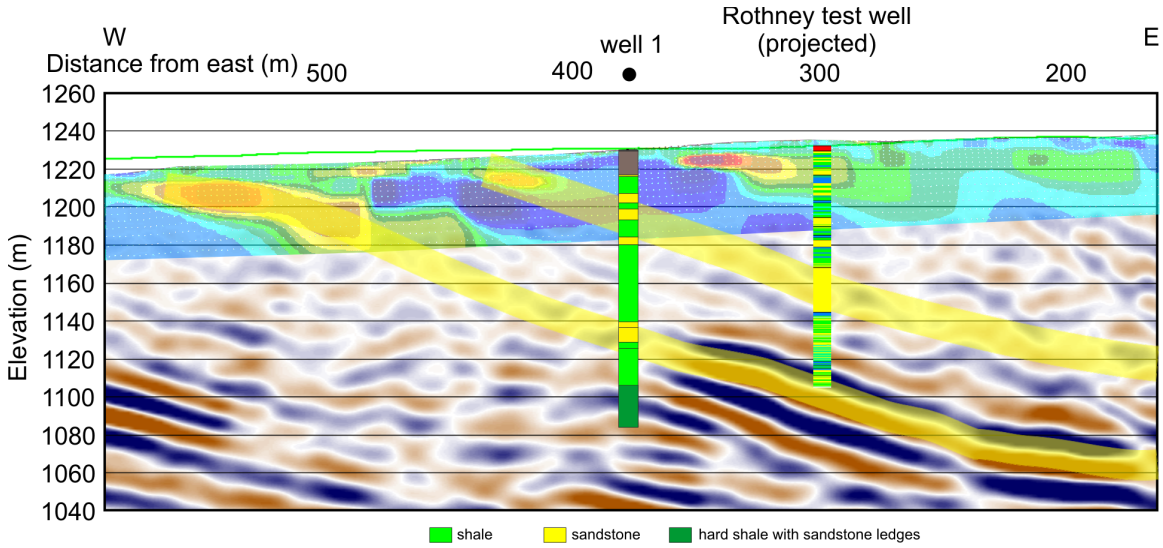

FIG. 11: Figure 10 with the lithology of well 1 overlain.

SUMMARY

The integration of seismic reflection data, a seismic refraction velocity model, inverted electrical resistivity data, and information from a nearby well allowed us to build an image of the near subsurface (<200 m) at Priddis, Alberta. We used the integrated data to predict the lithology to be encountered in a new well drilled in October, 2013. Our prediction of sandstones in the interval 25-50 m depth correlating to that penetrated by the Rothney observation test well was pretty good. Well 1 encountered grey sandstones from 23-28 m, 31-37 m and 46-50 m. A highly resistive body which correlated to high amplitude reflectors on the seismic data was predicted to be a sandstone and that it would be encountered at about 95 m depth. The well indeed entered a sandstone at 91 m. It also drilled with difficulty through a very hard layer at about 124 m depth. This we correlate to a strong reflection on the seismic data.

ACKNOWLEDGEMENTS

We thank the CREWES sponsors and Carbon Management Canada for their financial support. We also appreciate the software supplied by Landmark and GeoTomo.

REFERENCES

Geological Survey of Canada., 1941, Geology and structure cross-sections, Fish Creek, Alberta, Map 667A, scale 1:63,360.

Geotomo Software, 2013, RES2DINVx32/x64 – 2D resistivity & IP inversion software for Windows XP/Vista/7: www.geotomosoft.com/downloads.php

Isaac, J. H. and D. C. Lawton, 2010, Integrated geological and seismic site characterization at Priddis, Alberta: CREWES Research Report, **22**, 14p.

Loke, M. H., 2000, Tomographic modelling in resistivity imaging inversion: 62nd EAGE Conference and Technical Exhibition, extended abstracts, D-2.

Palmer, D., 1981, An introduction to the generalized reciprocal method of seismic refraction interpretation: Geophysics, **46** (11), 1508-1518.

Sasaki, Y., 1992, Resolution of resistivity tomography inferred from numerical simulation: Geophysics Prospecting, **40**, 453-464.

Wong, J., S. Miong, E. V. Gallant, H. C. Bland, L. R Bentley, and R. R Stewart, 2007, VSP and well logs from the U of C test well: CREWES Research Report, **19**, 12p.